

ESD ACCESSION LIST  
DRI Call No. 88345  
Copy No. 1 of 2 cys.

---

## Technical Note

---

1977-39

---

N. R. Trudeau  
B. Howland

### Design for High Accuracy Critical-Angle Sun Transit Sensor

20 October 1977

---

Prepared for the Department of the Air Force  
under Electronic Systems Division Contract F19628-78-C-0002 by

**Lincoln Laboratory**

MASSACHUSETTS INSTITUTE OF TECHNOLOGY

LEXINGTON, MASSACHUSETTS

---



Approved for public release; distribution unlimited.

ADA048287

The work reported in this document was performed at Lincoln Laboratory, a center for research operated by Massachusetts Institute of Technology, with the support of the Department of the Air Force under Contract F19628-78-C-0002.

This report may be reproduced to satisfy needs of U.S. Government agencies.

The views and conclusions contained in this document are those of the contractor and should not be interpreted as necessarily representing the official policies, either expressed or implied, of the United States Government.

This technical report has been reviewed and is approved for publication.

FOR THE COMMANDER

*Raymond L. Loiselle*  
Raymond L. Loiselle, Lt. Col., USAF  
Chief, ESD Lincoln Laboratory Project Office

MASSACHUSETTS INSTITUTE OF TECHNOLOGY  
LINCOLN LABORATORY

DESIGN FOR HIGH ACCURACY CRITICAL-ANGLE  
SUN TRANSIT SENSOR

*N. R. TRUDEAU*

*B. HOWLAND*

*Group 68*

TECHNICAL NOTE 1977-39

20 OCTOBER 1977

Approved for public release; distribution unlimited.

LEXINGTON

MASSACHUSETTS

## ABSTRACT

A sun transit sensor is used to detect the sun's passing a meridional coordinate plane of the satellite. Accuracy of operation of earlier sensors is limited by curvature of the fan beams associated with the critical angle prism. We describe a new, two-element critical angle prism assembly having the following properties: (a) curvature of the fan beam can be cancelled, or balanced against higher order terms, (b) reflection occurs at the interface between the glasses, (c) achromatism is possible.

A sensor utilizing two such prism assemblies operating in push-pull exhibits a planar fan beam having accuracy of  $\pm$  one arc minute over a sun latitude range of  $\pm 30^\circ$  (equatorial orbit requirement), or  $\pm 5$  arc seconds for sun latitudes of  $\pm 5^\circ$  (ecliptic orbit requirement). Equations governing the design, the choice of radiation resistant glasses, fabrication and testing will be discussed.

## TABLE OF CONTENTS

	<u>Page</u>
ABSTRACT .....	iii
I. INTRODUCTION .....	1
II. PRINCIPLE OF OPERATION OF THE TWO ELEMENT SENSOR ..	5
A. Conventional Prism Sensor .....	5
B. Two-Element Prism Sensor .....	10
C. Comparison of the Old and New Prism Assemblies .....	12
D. Measurement of the Accuracy of the Plane of the Sun Transit Sensor .....	12
III. DISCUSSION .....	22
IV. SUMMARY .....	24
APPENDIX -- ANALYTICAL TREATMENT OF THE SENSOR DESIGN .....	A-1
A. Description of the Grey Program .....	A-1
B. Instructions for the Use of the Grey Design Program .....	A-2
C. A Theoretical Digression: Choice of Glass Pairs .....	A-3
D. Sensor Design Optimized for Narrow Angle Operation .....	A-7
E. Design of the Gyro Drift Sensor .....	A-7
F. Grey Program .....	A-10
G. Sample Calculations from Grey Program .....	A-15

## DESIGN FOR HIGH ACCURACY CRITICAL-ANGLE SUN TRANSIT SENSOR

### I. INTRODUCTION

The Lincoln Experimental Satellite Program has generated requirements for a variety of solar sensors. We consider here the requirements for a planar fan-beam sun sensor, to sense the diurnal passage of the sun past the meridian (defined in satellite coordinates) of an earth-oriented synchronous orbitting satellite. This planar fan-beam sun sensor must indicate this meridian independent of satellite-sun orientation in elevation. Our sensor design is an extension of the method of Seward, whereby a critical angle prism sensor is used in a null circuit arrangement, to sense the transit of the sun across a meridian.

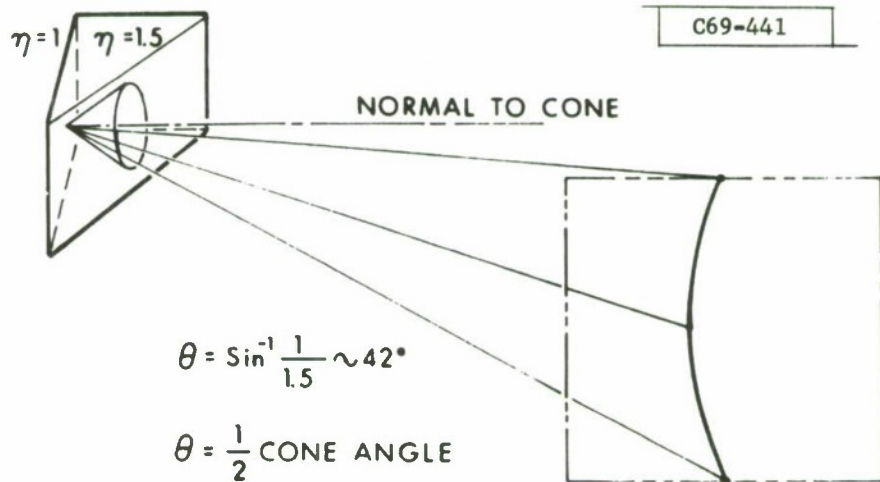
Early requirements for the LES-8 and -9 satellites specified an equatorial orbit, which would have necessitated a planar fan beam operating over a range of  $\pm 30^\circ$ . The subsequent change to an ecliptic plane orbit reduced this requirement to only  $\pm 5^\circ$ . The sensor described here is capable of arc-minute accuracy over the full  $\pm 30^\circ$  range, and accuracy of several arc-seconds over the more restricted  $\pm 5^\circ$  range.

The principal novel feature of the new sensor design, which utilizes two differing optical glasses, is that it permits the compensation of the inherent curvatures of the fan beams of the earlier critical angle prism sensor. The method of compensation requires, however, that we use

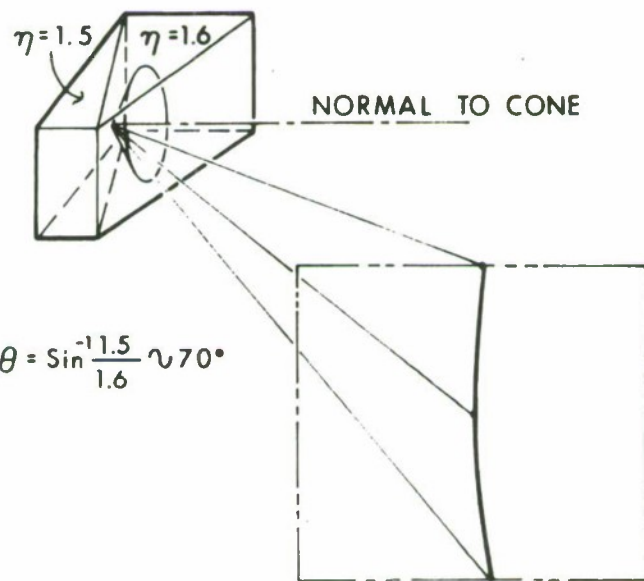
two glasses of differing indices; correct choice of these glasses vis a vis spectral dispersions also renders the sensor achromatic. Achievement of achromatism has two practical consequences: (a) it results in a more sharply defined fan beam, i.e., greater slope of the practical characteristic curves, and (b) it greatly facilitates operational testing of the sensor units, since an exact spectral match of the solar simulator and the sun is no longer necessary. (The latter advantage is probably the more important.) This method is illustrated qualitatively in Fig. 1, A and B. Here we show by an isometric projection fan beams generated by two pairs of optical media having large and small differences in refractive index. One sees that the smaller difference in indices yields a larger cone angle (indices of  $\eta' = 1.5$  and  $\eta = 1$  yield a total cone apex angle of  $83.62^\circ$  while  $\eta' = 1.6$  and  $\eta = 1.5$  yield a total cone apex angle of  $139.27^\circ$ ). A cone angle of  $180^\circ$  would represent a planar beam as well as zero aperture.

As mentioned earlier and shown in Fig. 1B, there is still residual curvature in the area of use of the sensor. This remaining curvature can be corrected or at least minimized by use of a prism. It is well known that a prism causes curvilinear distortion of a linear object. This is shown pictorially in Fig. 2. Instead of physically adding a prism to the sensor system, we can accomplish the same results by tilting the sensor surface, thus creating a virtual prism.

In summary, we were able to achieve a very good approximation to a planar fan beam sensor by utilizing total internal reflection at the



- A -



- B -

Fig. 1. Fan beam curvature due to conic section.

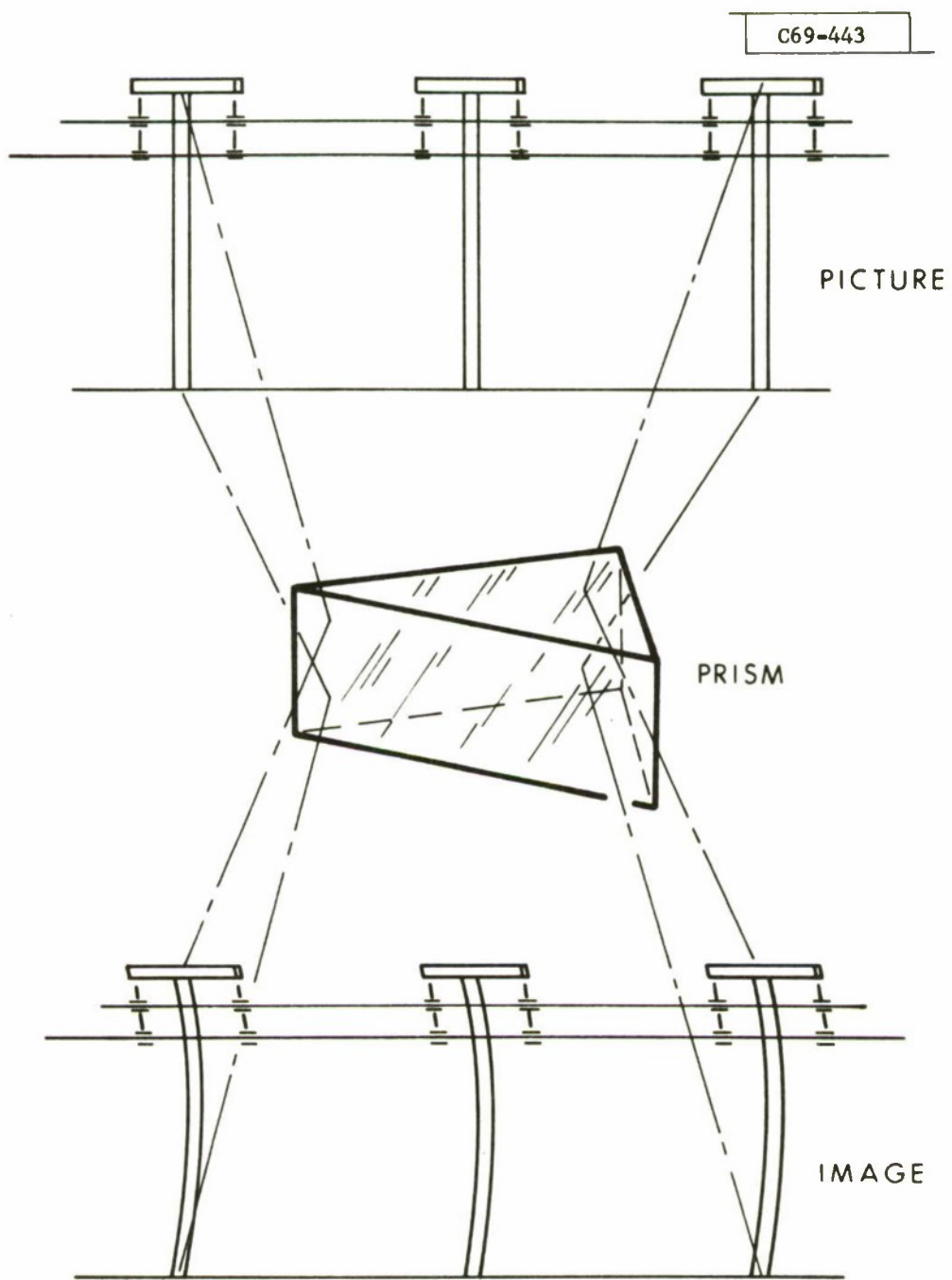


Fig. 2. Fan beam curvature due to prismatic effect.

interface of two glasses of nearly equal refractive indices, by tilting the sensor face, and by correct choice of the dispersions of the glasses so as to render the sensor achromatic.

Figure 3 shows, in pictorial form, the concepts and construction of the sensor. Figure 4 shows the diode current outputs versus sun angle, and Fig. 5 shows an expanded region of the curve of Fig. 4 about the coordinate center.

The two-element sensor is in practice fabricated as a cemented doublet. Accuracy considerations necessitated partial assembly before the final angles were ground into the outside surface. It is extremely important, however, to recognize that improper choice of the refractive index of the cement can cause fatal dysfunction of the device. Obviously the index of the cement should be chosen to be higher at all wavelengths than the lower of the two glass indices, if the performance of the sensor is to be governed by the indices and dispersions of the glasses, and independent of the index and dispersion of the cement.

## II. PRINCIPLE OF OPERATION OF THE TWO ELEMENT SENSOR

### A. Conventional Prism Sensor

In Fig. 6 we show, reproduced from the patent drawing, Seward's fan beam prism sensor, which provides the point of departure for our design. We will first discuss qualitatively the origin of the curvature of the fan beam, and will then show how it can be compensated.

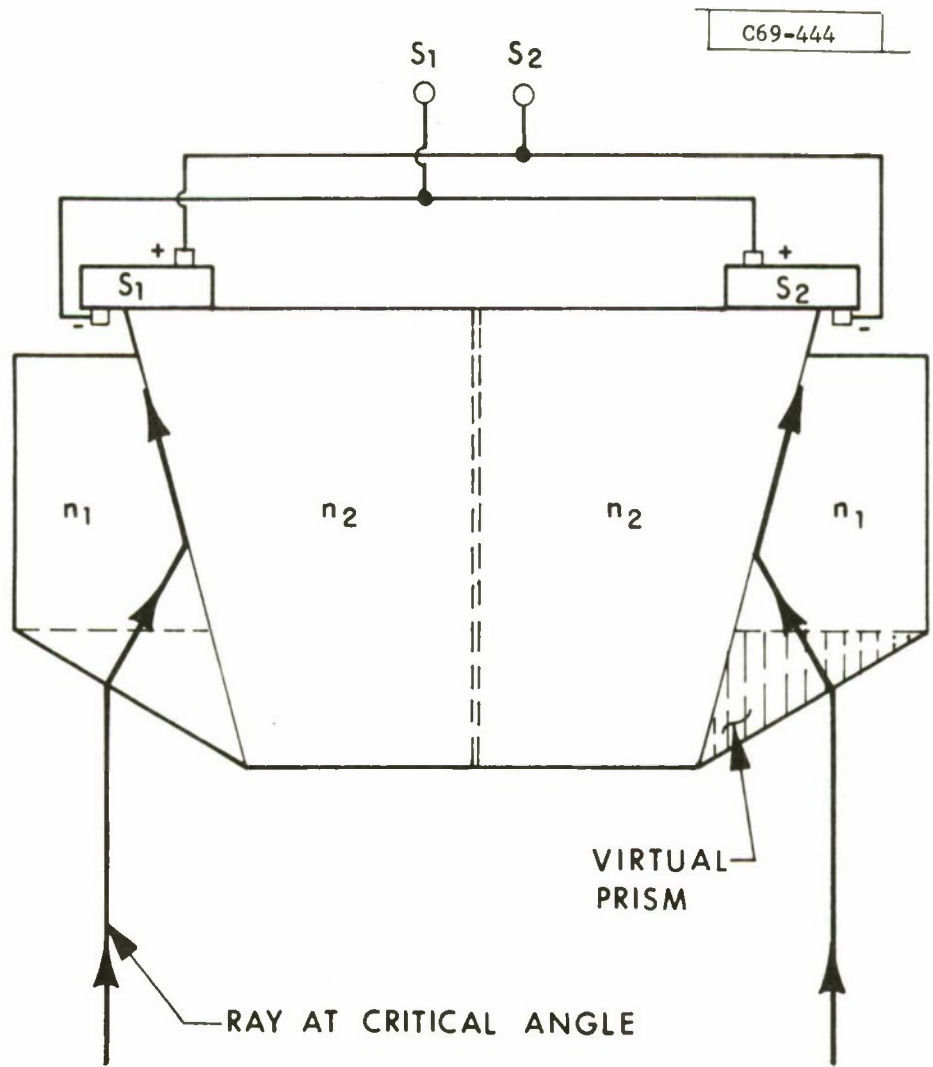


Fig. 3. Critical angle sun sensor.

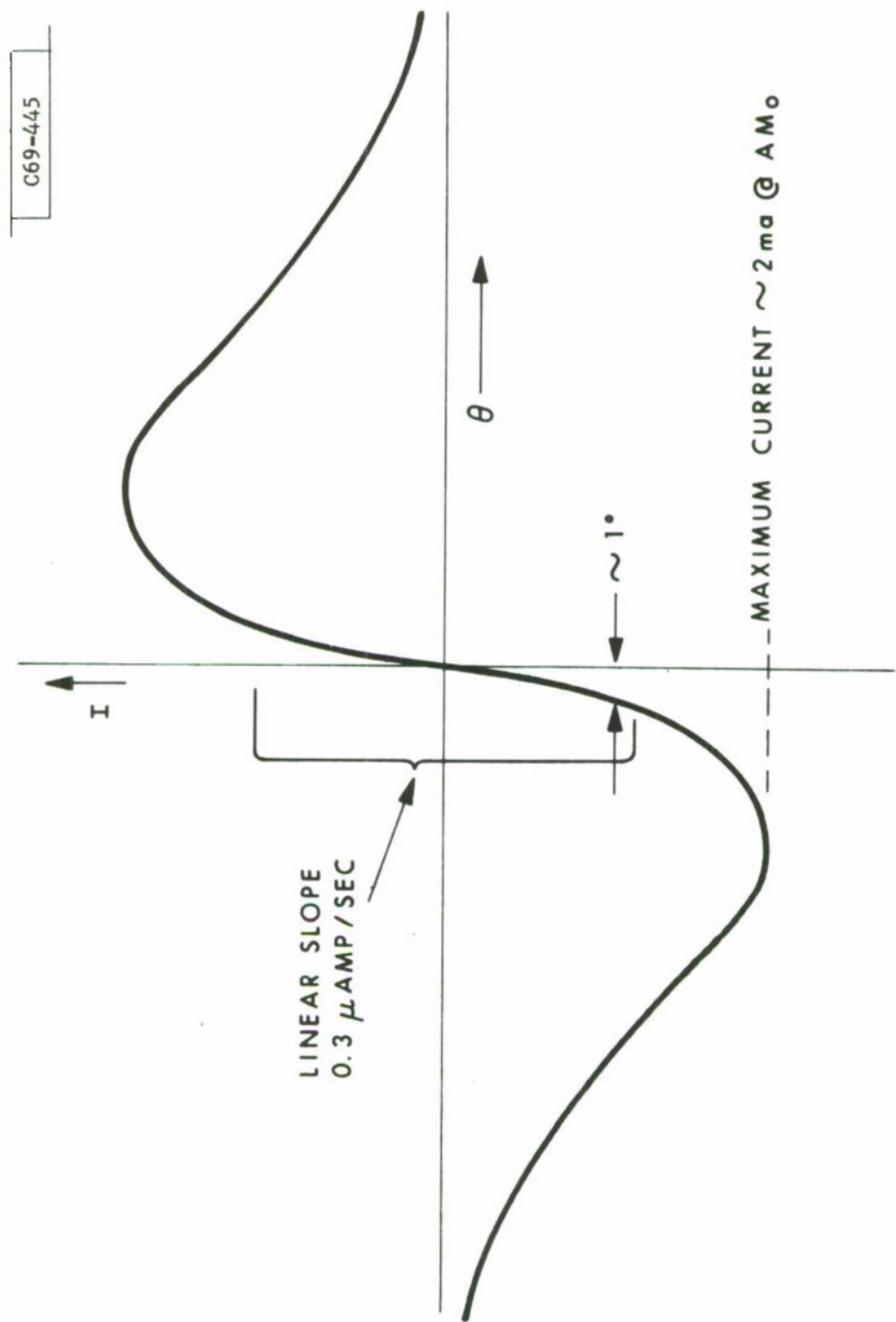


Fig. 4. Full transfer curve.

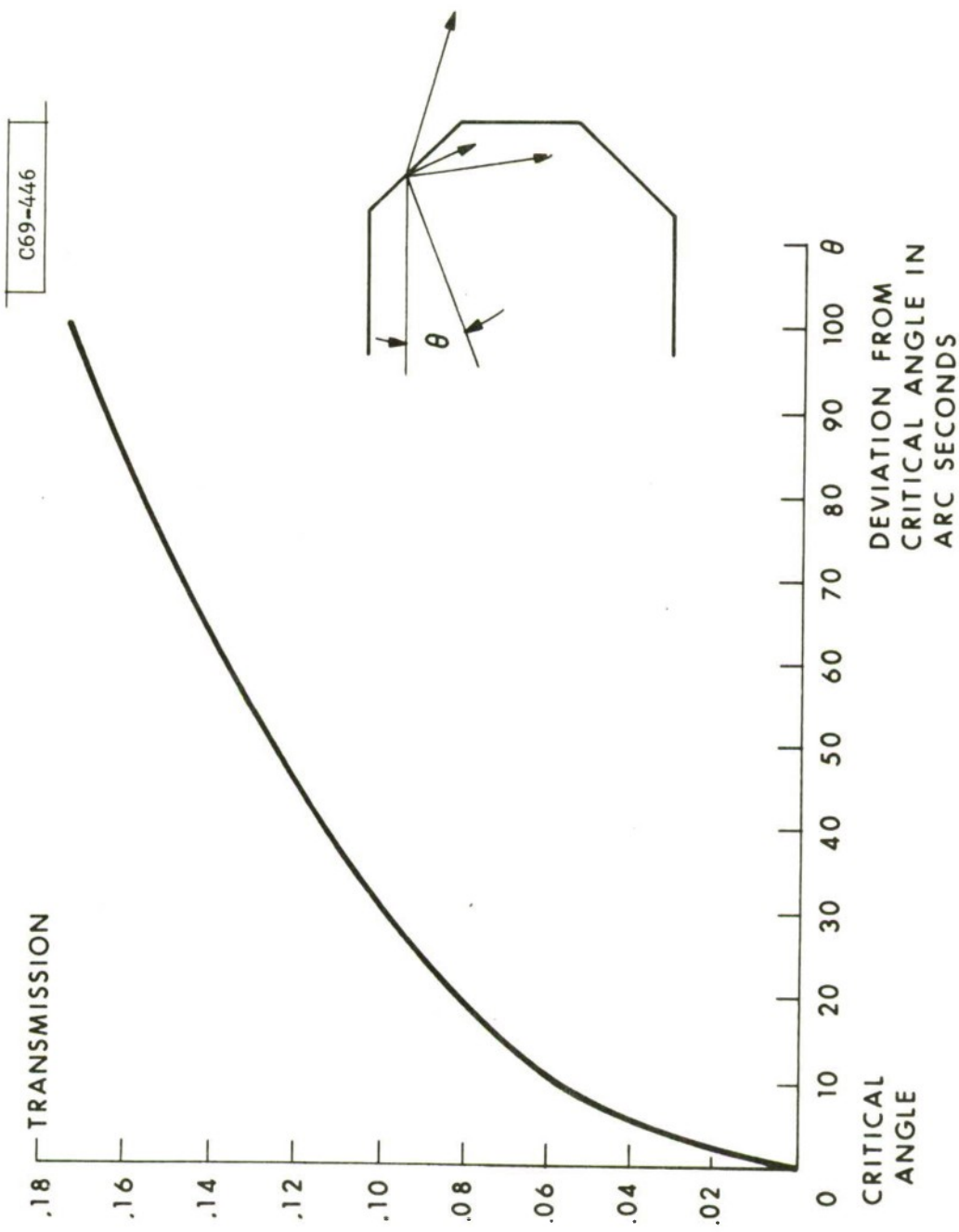


Fig. 5. Expanded transfer curve.

June 16, 1964

H. H. SEWARD  
3,137,794

DIRECTIONALLY SENSITIVE LIGHT DETECTOR

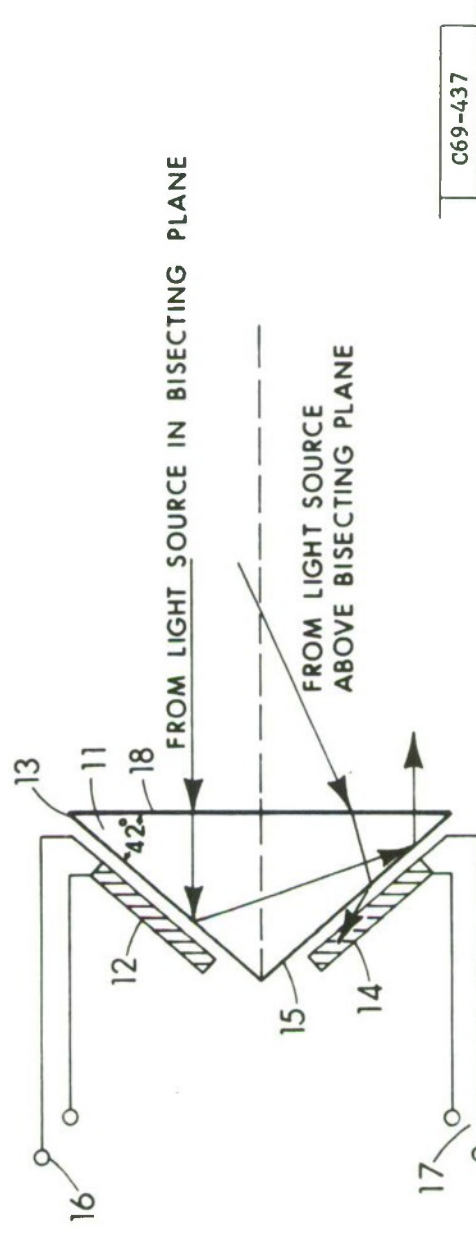


Fig. 6. Fan beam prism sensor — Seward.

It is well known that rays which pass internally in a glass and which encounter a glass-to-air surface can escape from the glass to the air only if their angles off the normal are smaller than  $\theta' = \sin^{-1}(\eta/\eta')$  where  $\eta$  is the index of refraction of the glass and  $\eta' > \eta$ . In Fig. 7 we show a cube of glass and a point  $P_1$  on the rear surface where light is assumed to exit. We now construct the cone which describes the locus of all the critical angle rays, i.e., those rays which are just capable of exiting from the glass. Note: These critical angle rays will, after exiting, travel parallel or very nearly so to the glass surface and any ray outside of this cone will be reflected back as if the rear surface were a mirror.

If we assume for the moment that the rays emanate from point  $P_1$  and we continue the rays away from  $P_1$  we now must encounter a second glass-to-air surface. In the figure, we show this second surface to be approximately normal to the meridional ray of the conical fan beam. Now, the internal set of rays defining the cone after exiting from this second surface will form a larger cone.

In the actual design of the sensor we use only the area indicated in Fig. 7. As can be seen, the locus of the critical angle rays must be straightened to yield a sensor which has an azimuthal angle which is independent of elevation angle, i.e., a planar fan beam.

#### B. Two-Element Prism Sensor

The two-element prism sensor makes use of two geometrical ideas to achieve a close approximation to a planar fan beam:

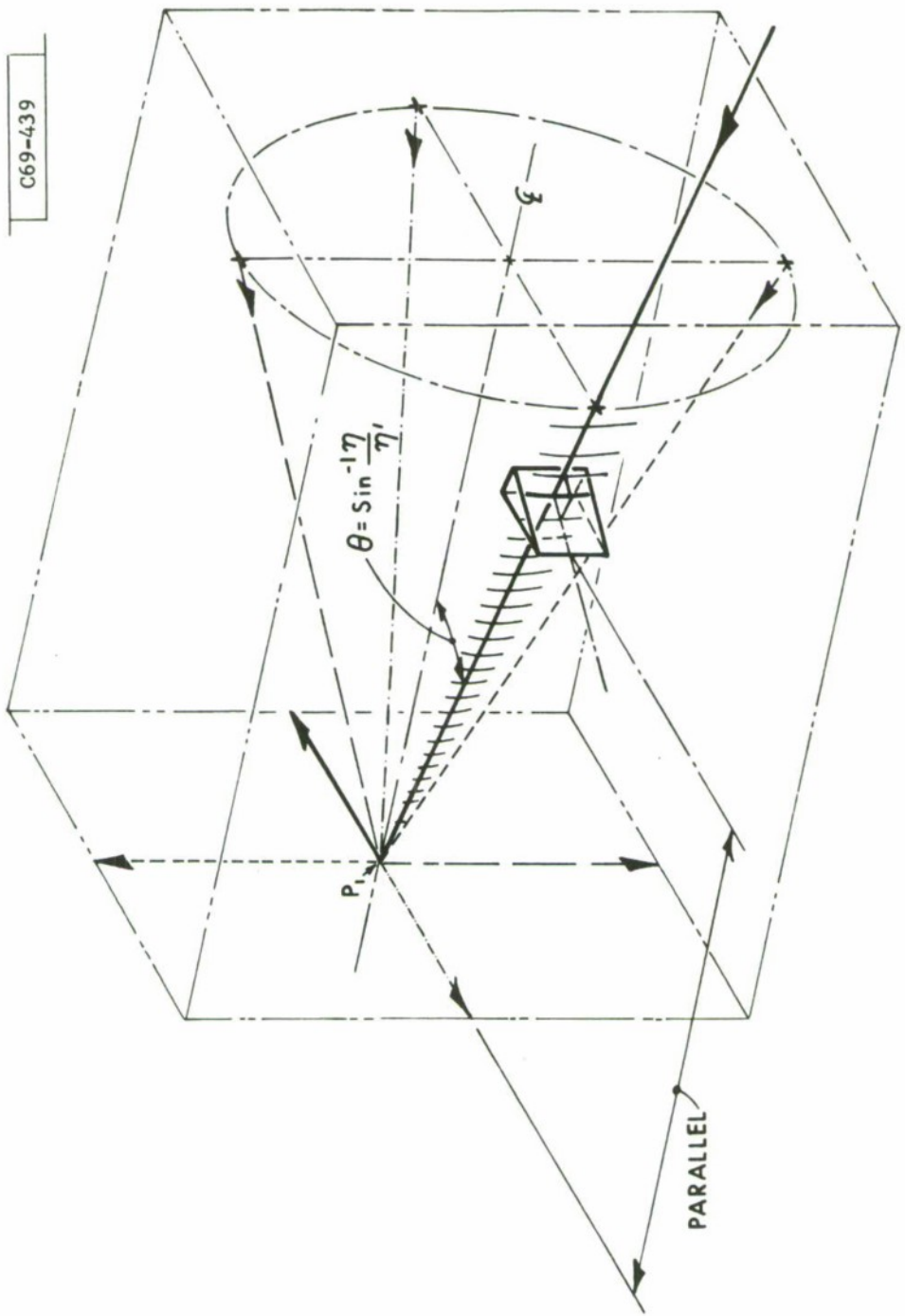


Fig. 7. Fan beam prism sectional view.

1. Glasses of only slightly differing indices of refraction are used to generate a critical angle cone of very wide apex angle, and

2. A virtual prism, realized by inclination of the surface face, is used to compensate the remaining curvature of the fan beams.

C. Comparison of the Old and New Prism Assemblies

In Fig. 8A and 8B we illustrate the operation of the old and the new prism assemblies, respectively; in each case we use paired solar cells to form a symmetrical assembly. We have here assumed the rays to emanate at the photocells, and show their projection on a fictitious plane, located some distance in front of the sensor assembly. In both cases, it is necessary to provide some overlap of the sensor fields of view, in order that they operate over a finite range of sun elevation angles and to make certain that no "dead-zone" occurs. This "toe-in" adjustment is to some extent provided for by the finite angular width of the sun. However, a computer program was used to convolve the sun's width and the necessary overlap to get the best response in terms of linear characteristic and output slope at the "null" crossing.

D. Measurement of the Accuracy of the Plane of the Sun Transit Sensor

The verification of the accuracy of the plane of the sun transit sensor has turned out to involve considerable effort, as there were several subtle difficulties which became apparent in early test results. These difficulties are listed in the order which they appeared and are discussed below:

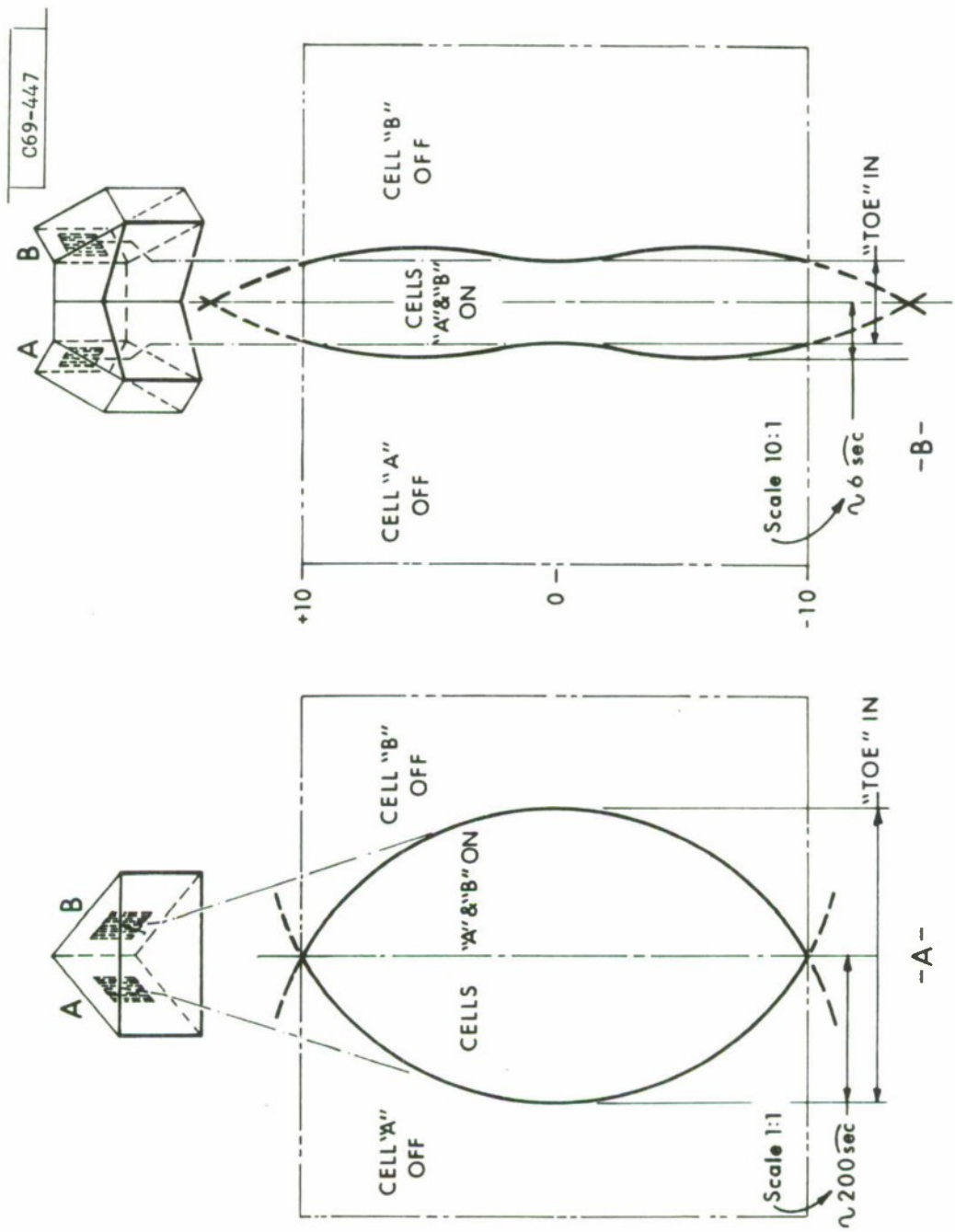


Fig. 8. Comparison of old and new design.

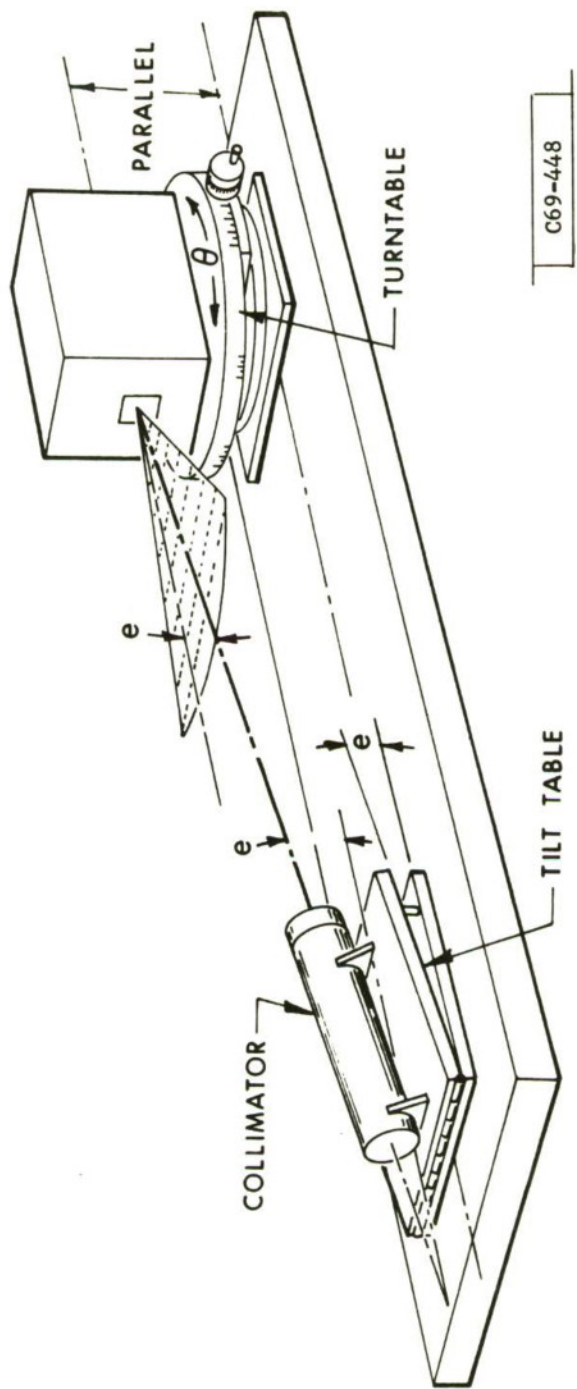


Fig. 9. Test station showing coning effect.

1. Difficulties due to reflections from the sunshades attached to the sensor.
2. Removal of coning errors due to misalignment of the axis of the light source and the plane of the turntable.
3. Irregularities in the light intensity and/or direction over the aperture of the collimating lens of the solar simulator.

Since the sensor actually takes a radiometric balance of all energy reaching the photodiode, it is very important that all stray light, and especially scattered light in close proximity to the sensor, be eliminated. Reflections from the sunshade, for instance, were fairly easily cured by the use of an inverted or backward sloping sunshade.

Removing of coning error required several measures. Figure 9 depicts the situation. Here we have assumed two compensating errors, as follows: the sensor is assumed to be misaligned by an angle,  $e$ , with respect to its housing, which is assumed to be accurately aligned to the plane of the turntable,  $T$ . The planar fan beam is parallel to the collimated light and can be adjusted by a precision angular tilt table to lie in the plane of the turntable. We assume that initially the source is at an angle of minus  $e$  with respect to the turntable.

Now, knowing these facts we can easily predict that the planar fan beam sensor will not stay in balance or "null" with rotation of the turntable, since the shape of beam which would be required for balance would be that of a cone with apex angle of  $(180 - 2e)$  degrees. Such a cone is easily shown to depart from the planar fan beam by angles given to a close approximation by  $d = (1 - \sin \theta)e$  where  $\theta$  is the horizontal angle of slewing of the table. Once we had determined that this situation could occur, we devised methods for its neutralization.

The angles of the sensor and the tilt table governing the collimated solar source can be iteratively adjusted so as to reduce the parabolic or coning error to zero. This method has the disadvantage that it entirely prevents us from determining if the sensor itself has an inherent parabolic error.

The solar source can be aligned by means of a precision theodolite, mounted on the surface plane supporting the turntable, sensor, etc. Such an alignment has the disadvantage that it is insensitive to variations in the effective center of gravity of the solar source, such as would be caused by uneven distribution of light across the filament.

A method which obviates the need for the precision theodolite, and which has some interesting features, utilizes a Master Precision Sensor. See Fig. 10. Here we have mounted a larger version of the sun transit sensor in a highly precise rectangular block. This external housing contains provisions for accurate and stable adjustment of the angular orientation of the sensor in two directions with respect to the external surface of the housing. Note: The method requires that the housing be square to gauge-block accuracy.

To determine the exact radiometric center of the source requires the iterative adjustment of the angular alignment of the sensor with respect to the block, and the light source with respect to the plane of the turntable.

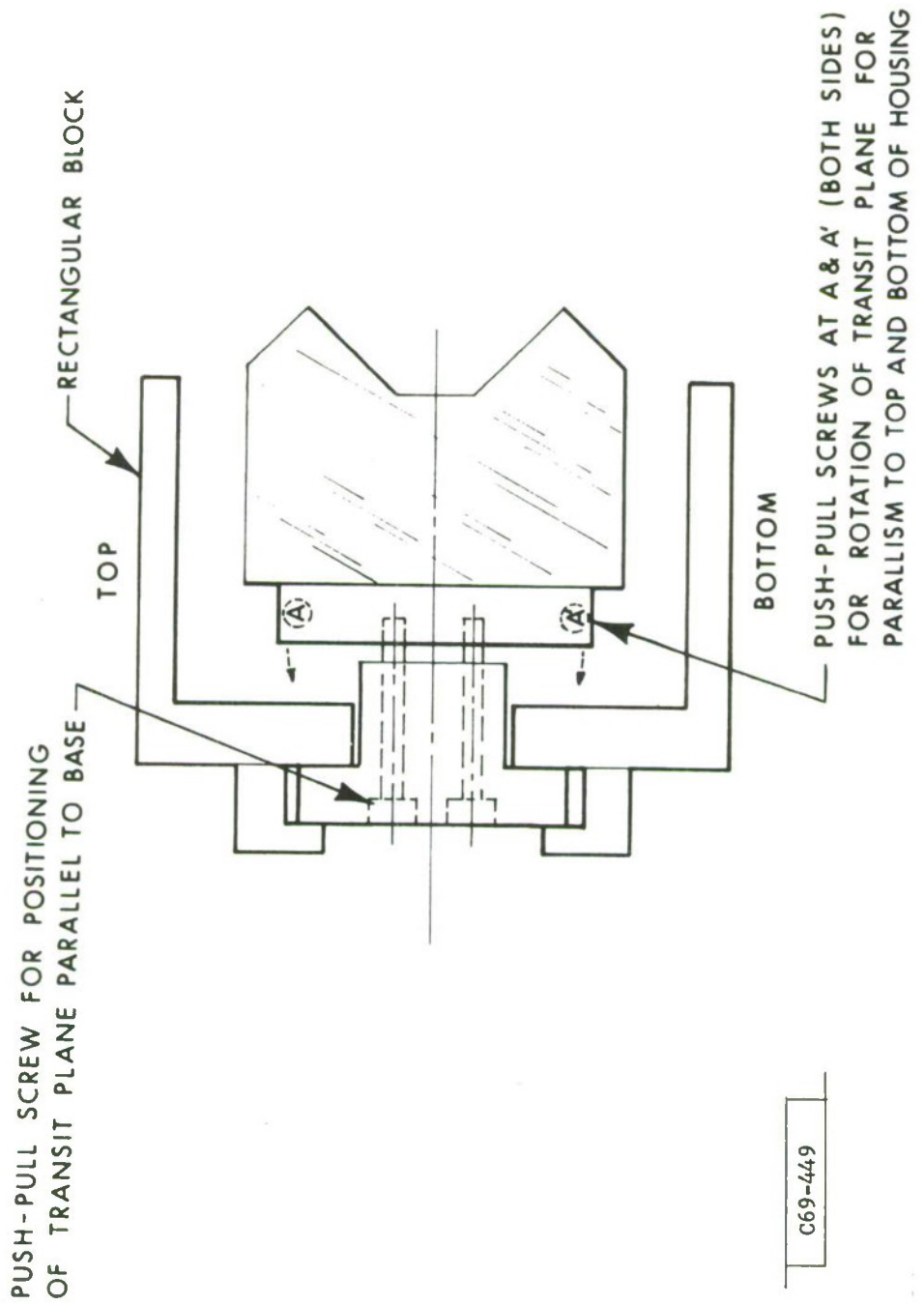


Fig. 10. Master precision sensor.

First, the sensor is placed on the turntable with the planar fan beam horizontal. The solar source azimuth is then set to zero by retro-reflection (this is not critical). The solar source elevation is then adjusted by a 0.0001" micrometer for a "null" or zero current from the diode and the micrometer reading is recorded.

Then the sensor is rotated 180° about the line extending towards the source, i.e., it is turned upside down, and the solar source is again adjusted for "null", and the micrometer reading again recorded.

The two micrometer readings determining the solar source elevation are averaged and the micrometer is then reset to this new position. The sun transit sensor is then adjusted in its mount to achieve a null at this new source position.

The sensor is then rotated in azimuth to its plus limit value, and the sensor output will in general go out of null. The null is restored by adjustment of the plane of the transit sensor with respect to its precision mount, i.e., by rotation about the axis pointing to the source. Proper adjustment is indicated when a null reading is attained for the same solar elevation reading at the plus and minus azimuthal limit settings.

Finally, since all these adjustments interact somewhat, they must be iterated and their settings locked when no further improvement is possible.

Now, it is still possible to go wrong with this procedure, due to non-uniformity in the solar source. However, the procedure is interesting

in that it shows that the combination of a sensor, and the precision housing (which we have termed the Master Precision Sensor) is in principle self-calibrating, and self-checking. Thus, the sensor itself determines the center of gravity of the solar source.

The two remaining elements of the calibration setup are turntable and light source. The turntable used for sensor calibration utilized two optical flats with an extremely thin coating of oil between them. For the tests at Draper Laboratory with the Gyro package, a large size Ultradex rotary table, guaranteed to two arc second accuracy, was then used to check the alignment of the sensor within the Gyro package.

The element of the test system which gave most of the difficulties was the solar source. The source which we first used for our tests was a 15-watt tungsten light bulb designed for microscopy having a compactly wound 3 mm x 4 mm rectangular filament coupled with a 300 mm focal length lens. The chamber housing the bulb was air cooled, and the bulb voltage was adjusted by an autotransformer.

The difficulty with this scheme, which resulted in a series of unreliable and unrepeatable measurements, was traced to the combination of: (1) the unevenness of light over the aperture of the telephoto lens, and (2) azimuthal rotation of the sensor about an axis which was displaced an unrecorded amount towards or away from the light source. This had the effect of translating the sensor across the aperture of the solar source as the azimuthal angle was varied. Now, it could be argued that

we know where the aperture of the sensor was located, and thus it could be set coincident with the axis of the turntable. But, due to the multiple apertures of the sensor, formed by the sunshade, the solar cell detectors, etc., we could not in fact be sure of the location of the aperture, that is, its effective position as viewed from the front of the sensor. Moreover, there was obviously something inherently unsatisfactory with a test procedure which would operate only when the device under test was located within a few millimeters of a given spot, since there existed no way of independently verifying that the sensor was so located.

Accordingly, we sought and determined what was causing the unevenness in the illumination of the solar source: (a) multiple reflections within the multi-element telephoto lenses, and (b) unevenness in the tungsten filament when viewed from different directions. To solve (a), we used a large aperture Nikon 300-mm f/4.5 lens which was stopped down to f/5.6 or f/8. This lens, operating at a distance of 12 to 16 inches from the sensor, was determined to have negligible internal reflections. It would probably have been still better to use an achromatic doublet as the collimating lens with effective internal baffling.

The problem with the tungsten filament source was determined to be Moire-type shadowing of some of the wires of the wound filament by others. An effort to substitute ribbon type filaments was unsuccessful; instead the light source was redesigned using a fiber optic light guide and illuminator, as shown in Fig. 11. Here we have used a conventional quartz-iodine fiber-optical light projector to illuminate a 1/8-inch diameter fiber-optic

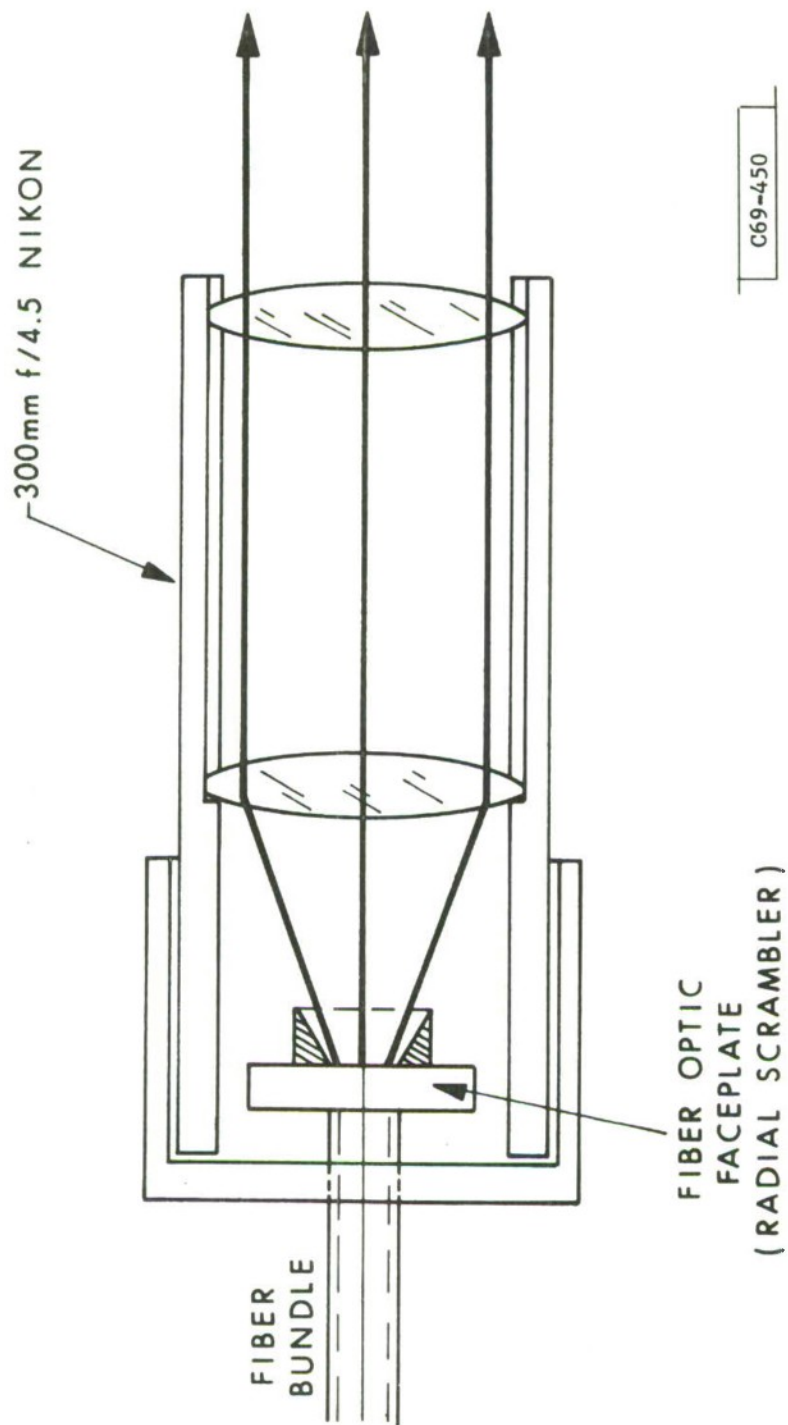


Fig. 11. Fibre optic illuminator.

light guide, which is terminated with a precision 3 mm aperture (matching the 300 mm focal length of the lens to the solar diameter), together with a fiber-optic faceplate diffusing screen. This screen is the key to the success of this method.

It must be realized that many conventional flexible fiber optic light guides are of highly imperfect construction: the fibers at the termination do not all intersect the axis of the termination of the guide at the same angle. Thus one can easily see irregularities in the light distribution over the aperture of the circular tip, if one looks from differing angles off the axis. This would have led again to highly non-uniform illumination over the aperture of the collimating lens. However, the fiber optic diffusing screen restores the circular symmetry of the directionality of illumination of the beam, and thus effectively "homogenizes" the beam over the aperture of the lens. The projector is chosen to completely fill the angular aperture of the light guide at its proximal end to permit even radial illumination of the aperture of the collimating lens, which is checked visually with a ground glass screen, for the presence of spurious foci and gross abnormalities.

With these modifications to the original light source, we were able to make repeatable measurements of the gyro sun transit sensors to one or two arc seconds accuracy; the complete setup is shown in Fig. 12.

### III. DISCUSSION

Most of the problems described above were due to a failure to appreciate the difficulty of certifying the operation of a sun sensor to

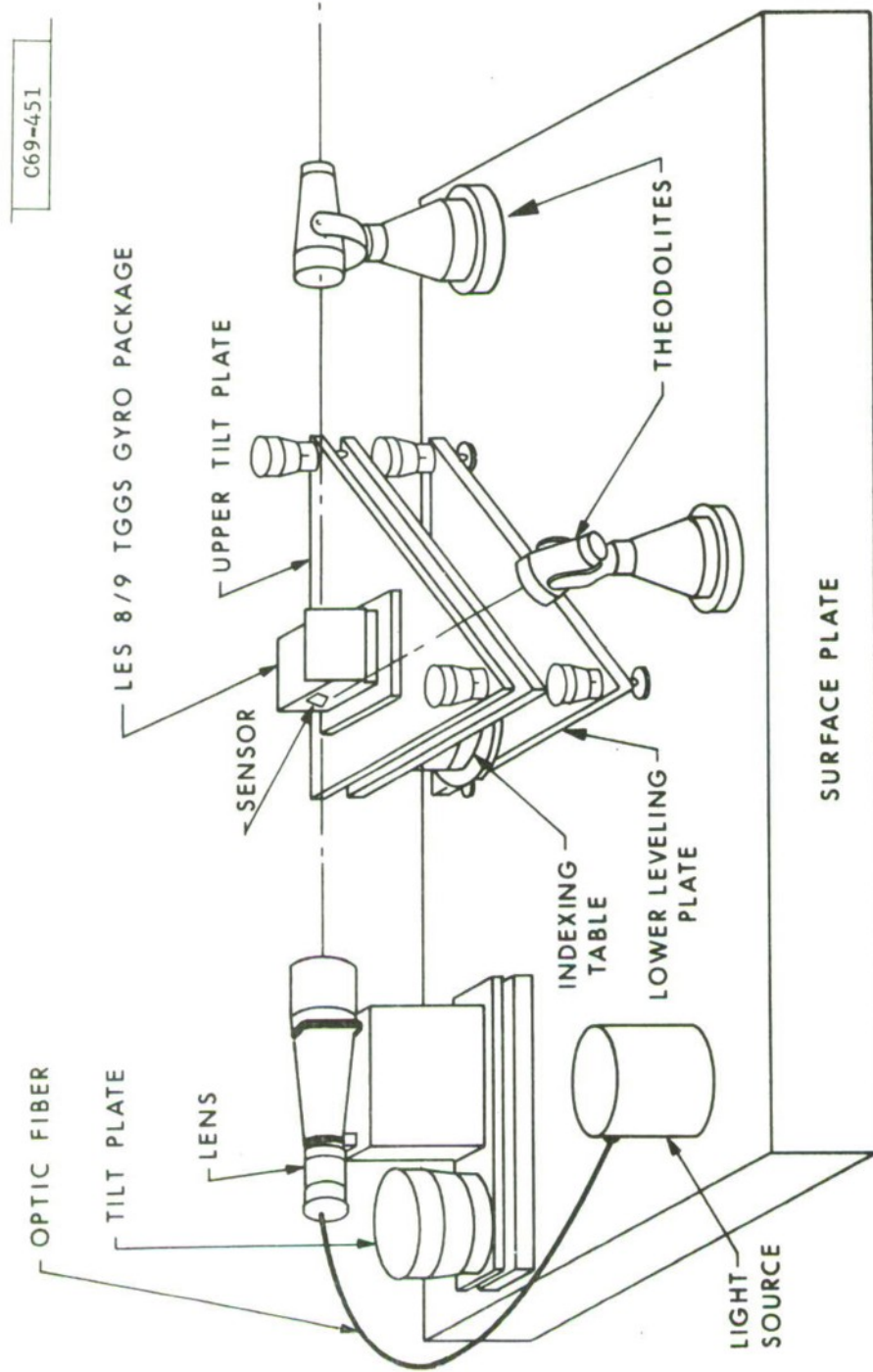


Fig. 12. Final test station.

arc-second accuracy. In particular, the design of a small aperture, low-power solar source having very modest power and cooling requirements, is not an easy task. Further, the choice of a multi-element camera lens as the collimating lens was unfortunate because of the multiple reflections in all such lenses, which tend to cause spurious focal spots along the axis (Boyes points).

Future work will put more effort into the solar simulator. The present sun transit sensor is, we believe, a very sensitive test instrument with which to verify the quality of a solar simulator.

#### IV. SUMMARY

The original sun transit sensor (U.S. Pat. #3,137,794) utilizes the properties of a symmetrical, critical angle prism assembly to achieve sun transit sensing in the equatorial plane of a satellite. This device has, however, two shortcomings: the critical angle, since it is a function of the index of the glass, varies with wavelength and sensor operation out of the equatorial plane is compromised by the curvatures of the mathematical surfaces defining the null responses of the photosensors.

An improved, two-element prism sensor has been realized which is both achromatic and compensated for the first-order curvatures of the surfaces defining the null response. Two such prisms, symmetrically disposed, with an optional toe-in adjustment comprise the improved sensor assembly. The design of this new sensor element requires some care, since once the indices of the two glasses are chosen, their dispersions must be in a set

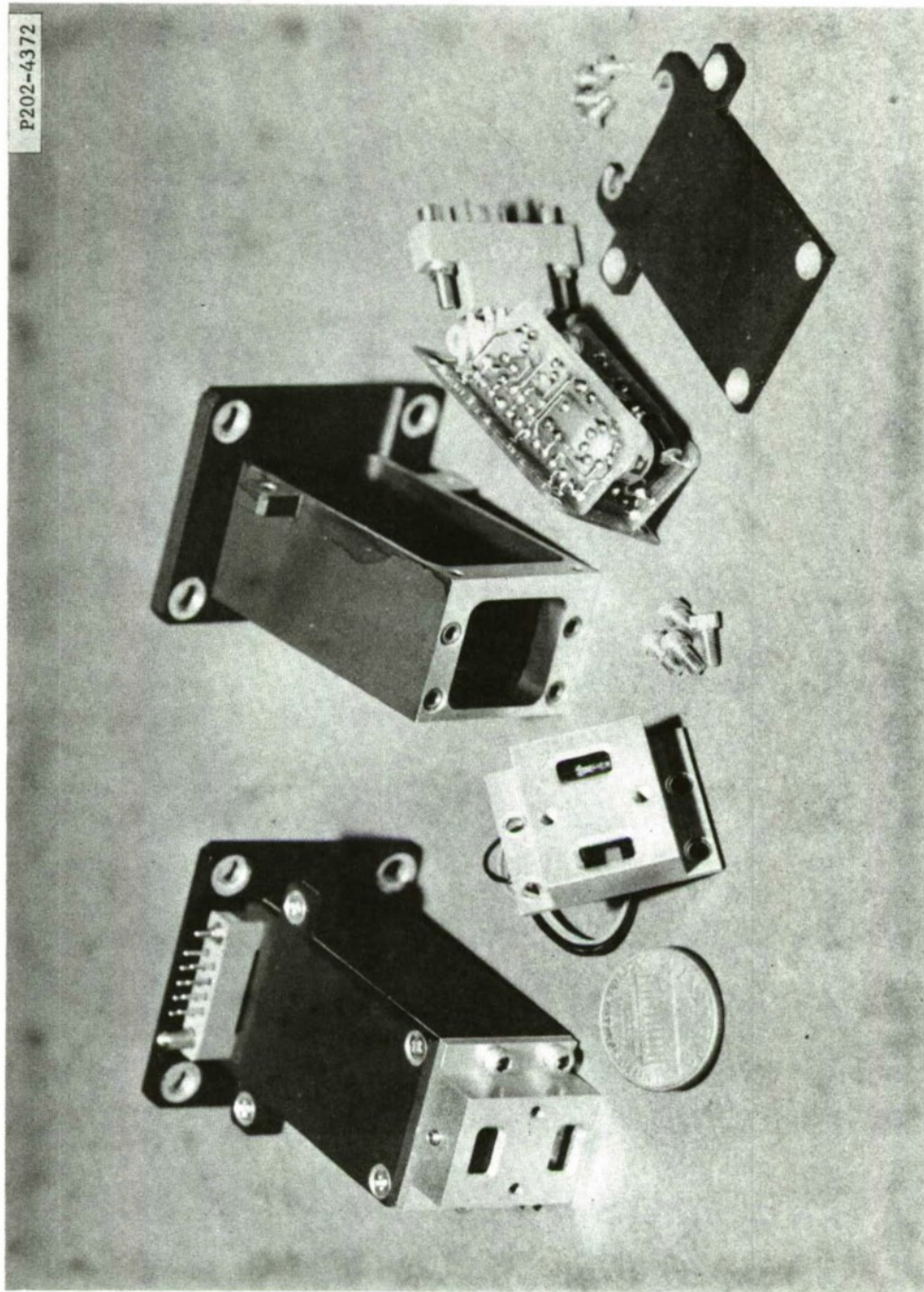
ratio. A graphical method for selecting from a large compatible glass pairs and an analytical method for designing the prism half cell having zero fan-beam curvature are given in Appendix I. The practical designs (Figs. 13, 14, and 15) used in the LES-8/9 satellites were, however, realized with the aid of the Grey design program,\* which permits optimal performance over a prespecified range of azimuthal angles, by balancing fourth order curvatures with small amounts of parabolic curvatures. This results in four-fold reduction in total error over the zero-curvature case. Using the limited selection of available radiation resistant glasses, several compatible pairs of glasses were obtained which resulted in satisfactory designs. Half-cells using these designs have errors on the order of a few arc minutes for a plus or minus  $30^{\circ}$  sun elevation angle--a range characteristic of an equatorial orbit -- and as many arc seconds error for the  $\pm 10^{\circ}$  range sufficient for an ecliptic orbit. By using two half-cells in a symmetrical, push-pull design the error of the sensor should be at least an order of magnitude better. We may state that the inherent error of the sensor is of little practical consequence in the case of the equatorial orbit, and of no consequence in the ecliptic orbit ( $\pm 10^{\circ}$ ).

Practical realization of the sensor, and verification of the theory, have been described, and designs for the critical gyro-sensor package have been built and tested.

---

\* Prepared for us by the David Grey Associates.

Fig. 13. Critical angle sensor used in stationkeeping system.



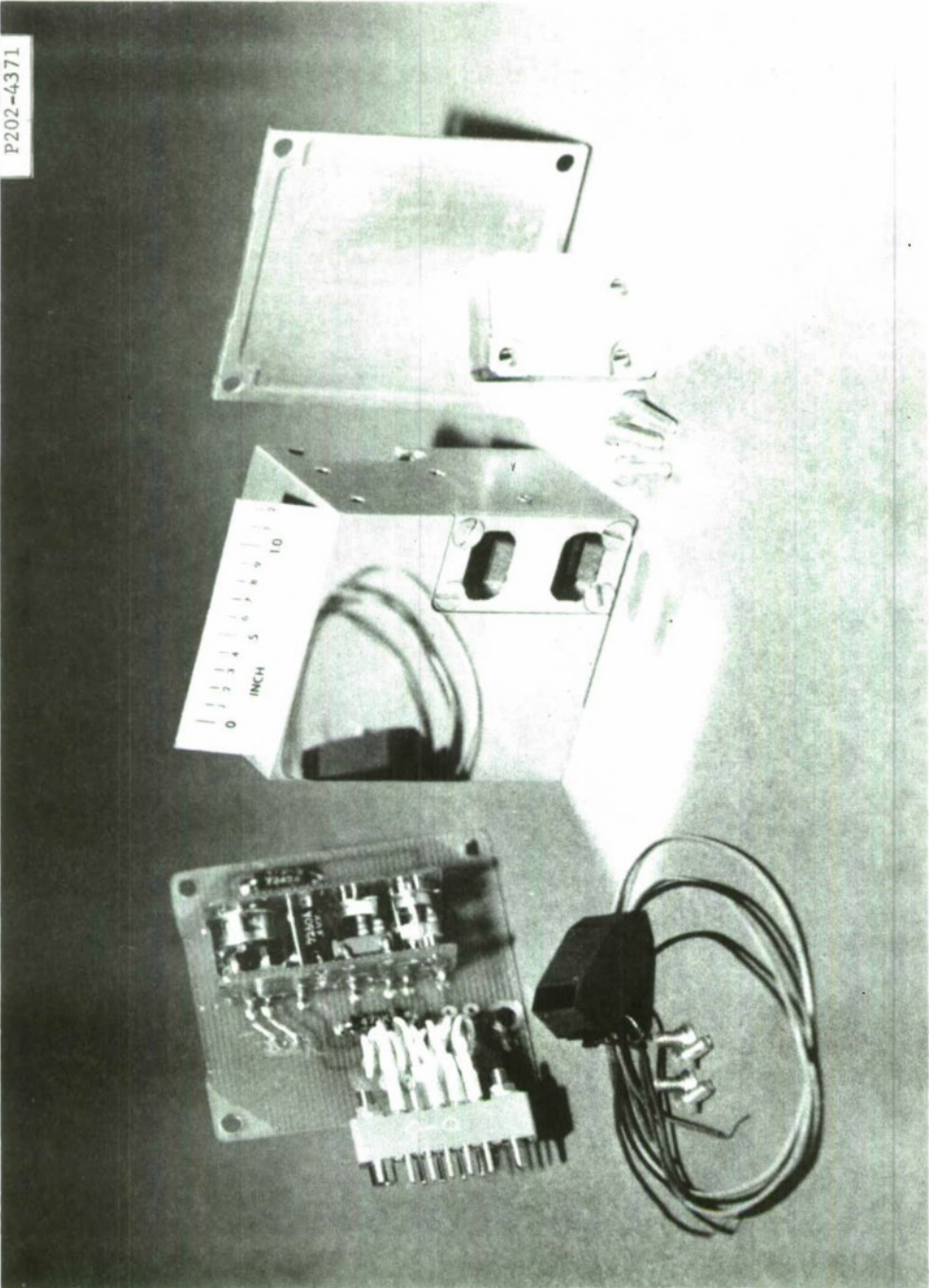


Fig. 14. Critical angle sensor used in gyro system.

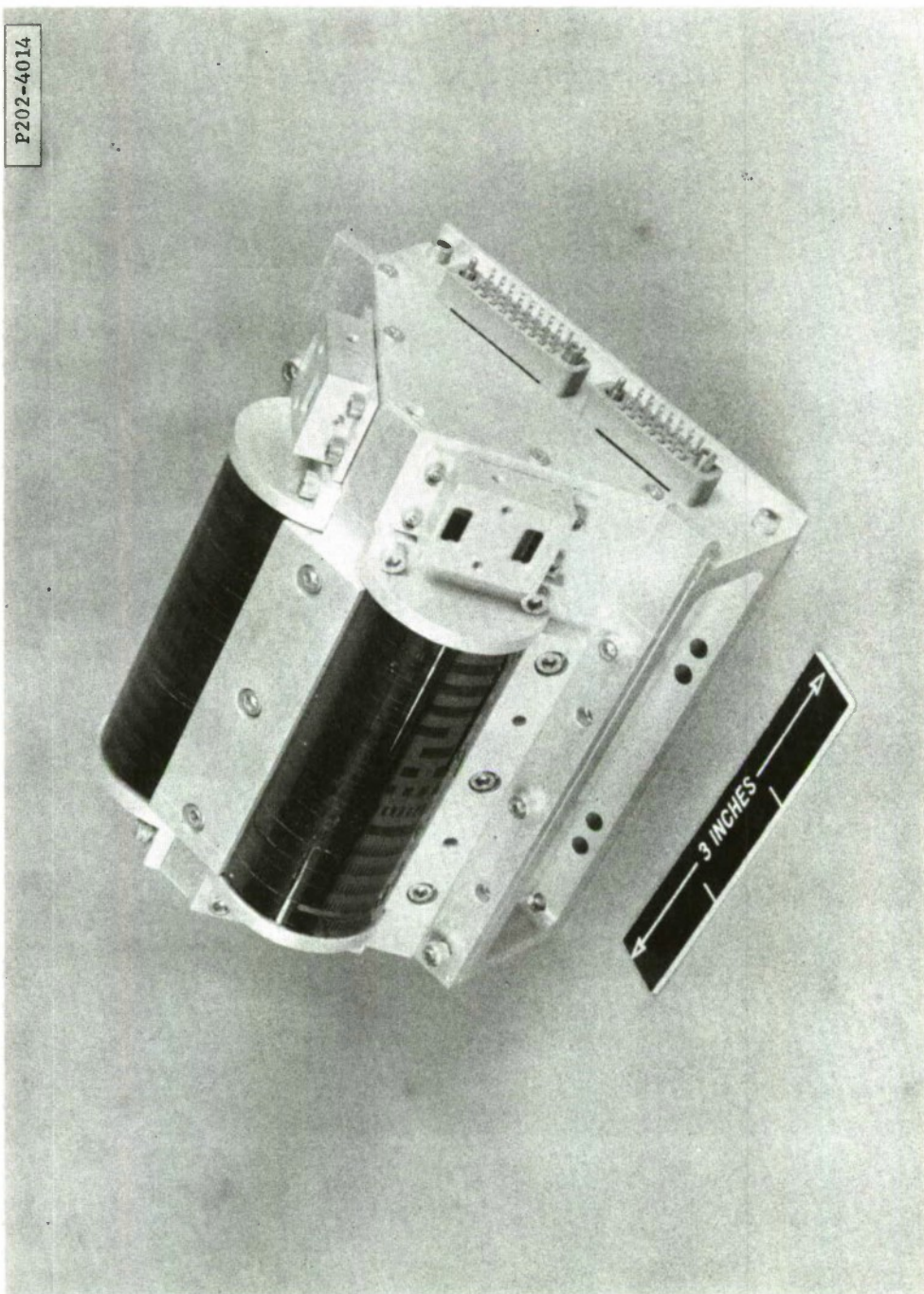


Fig. 15. Critical angle sensor (Section A) used in orbit fitting system.

Further work to perfect the measurement methods and to determine the residual errors and eliminate the practical errors inherent in the arc-second range is indicated.

## APPENDIX

### ANALYTICAL TREATMENT OF THE SENSOR DESIGN

#### A. Description of the Grey Program

There is a trade-off in the design of the two-element sensor between accuracy of the planar fan beam and the range of sun elevation angle over which the sensor will operate. We consider here the question: with available optical glasses, how do we design the sensor for greatest accuracy of the planar fan beam for a given range of sun elevation angle?

In order to solve this problem, we called on David Grey Associates, who designed for us an optimization program. This program, with some recent revisions and added documentation, is listed at the end of this Appendix. The Grey program solves completely the analytical design problem, in that it determines the optimal angles of the prism assembly for specified glass types.

We shall describe the operation of this program in detail and give some important results. We have also attempted an analytical treatment of the geometrical problem for the sensor, with two further results: (a) we have developed a formula which preselects the glass pairs for achromatism, and (b) we have a solution for the design of the zero curvature fan beam sensor. The latter special case does not, of course, result in the smallest mean square error over a range of sun elevation angle.

B. Instructions for the Use of the Grey Design Program

The Grey program determines the optimal angles of the prism assembly, when supplied with the correct input data. Two data cards are required for each glass pair for which a design solution is desired. The first data card specifies the indices and dispersions of the pair of glasses. The second card permits the specification of as many as six angles, with six default options; the program will operate if this card is inserted but left blank.

The glasses are specified as follows: the index of the first glass, its dispersion, the index of the second glass and its dispersion. If either index is omitted, the program writes "fatal data default" and goes on to the next glass pair. Other options are the following: (1) If the glasses are entered in the wrong order, the program interchanges them. (2) If the dispersion of the higher index glass is omitted, the program assumes it to be 100. (3) If the dispersion of the lower index glass is omitted, the program computes the optimal dispersion for achromatic correction, and uses same. (4) If it is entered, the optimal dispersion is computed nonetheless, but the supplied dispersion is utilized. There is room on the glass card for a title describing the glass types.

The second data card supplies various angles, by far the most important of which is the CV(2), the angle specifying the sun elevation angle for which correction is achieved. That is, the sun azimuthal error will be adjusted to be zero for this sun elevation angle by changes in the prism angles; this optical correction is achieved by balancing second and

fourth order curvatures in the characteristic. The use of this balancing technique results in an approximately four-fold reduction of total error, over a design which chooses zero curvature of the fan beam at the equatorial plane of the sensor.

A further option (5) is to specify the angles of the prism directly, as CV(5) and CV(6), thus permitting the solution of non-optimal prism assemblies, such as were originally used, to compare theory with experiment. Both prism angles must be entered to effectuate this option. Further angles entered on the second card are the fan beam interval, CV(4), the fan beam cut-off angle, CV(3), beyond which we do not compute, and starting angle for the interaction sequence, CV(2).

The program prints out the optimal design angles of the prism, and then prints a table of the azimuthal error of the half cell of the sensor, versus the elevation angle of the fan beam in air. (All such angles are measured in degrees.) The program then increments to a second wavelength, here approximately 950 nanometers (if the indices given were for the sodium D-line,  $\eta_D$ ) and the recomputes the error table.

#### C. A Theoretical Digression: Choice of Glass Pairs

Since the Schott catalog contains over a hundred optical glasses, it is impractical to test all pairs for their chromatic match in the sensor design. Instead, we will preselect the glass types, so that the Grey program can be used more efficiently. The selection that we require is that, given indices

$\eta_1$ ,  $\eta_2$  and dispersions  $J_1$ ,  $J_2$ , respectively, that the sensor will be achromatic when

$$J_1 \left( \frac{\eta+1}{\eta} \right) = J_2 \left( \frac{\eta^1+1}{\eta^1} \right) = K \quad (1)$$

The above relation serves to define the parameter  $K$ . Thus, if glasses are plotted on the  $J$ ,  $\eta$  plane as is customary, two glasses will be compatible, i.e., result in an achromatic sensor if they lie on the same curve of the set of curves generated by the parametric equation:

$$J^* = \left( \frac{\eta^*}{\eta^*+1} \right) \cdot K^* \quad (2)$$

These curves are easily shown to represent a family of equiangular hyperbolas, each curve having asymptotes at  $J = K^*$  and  $\eta^* = 1$ .

This situation is illustrated in Fig. A-1, wherein we show plotted the twelve Schott radiation resistant glasses. It is seen that all the glasses, except for three, lie on widely separated hyperbolas. Thus, only three such achromatic sensors can be constructed from this set of twelve glasses. These use the three possible glass pairs as follows: GG-375-G vs. SK-4G, GG-375-G vs. BAK-1G and BAK-1G vs. SK-4G.

In Fig. A-2, we show the results of a pair of glasses, at the primary color, with a  $30^\circ$  crossover point. There is a slight advantage by

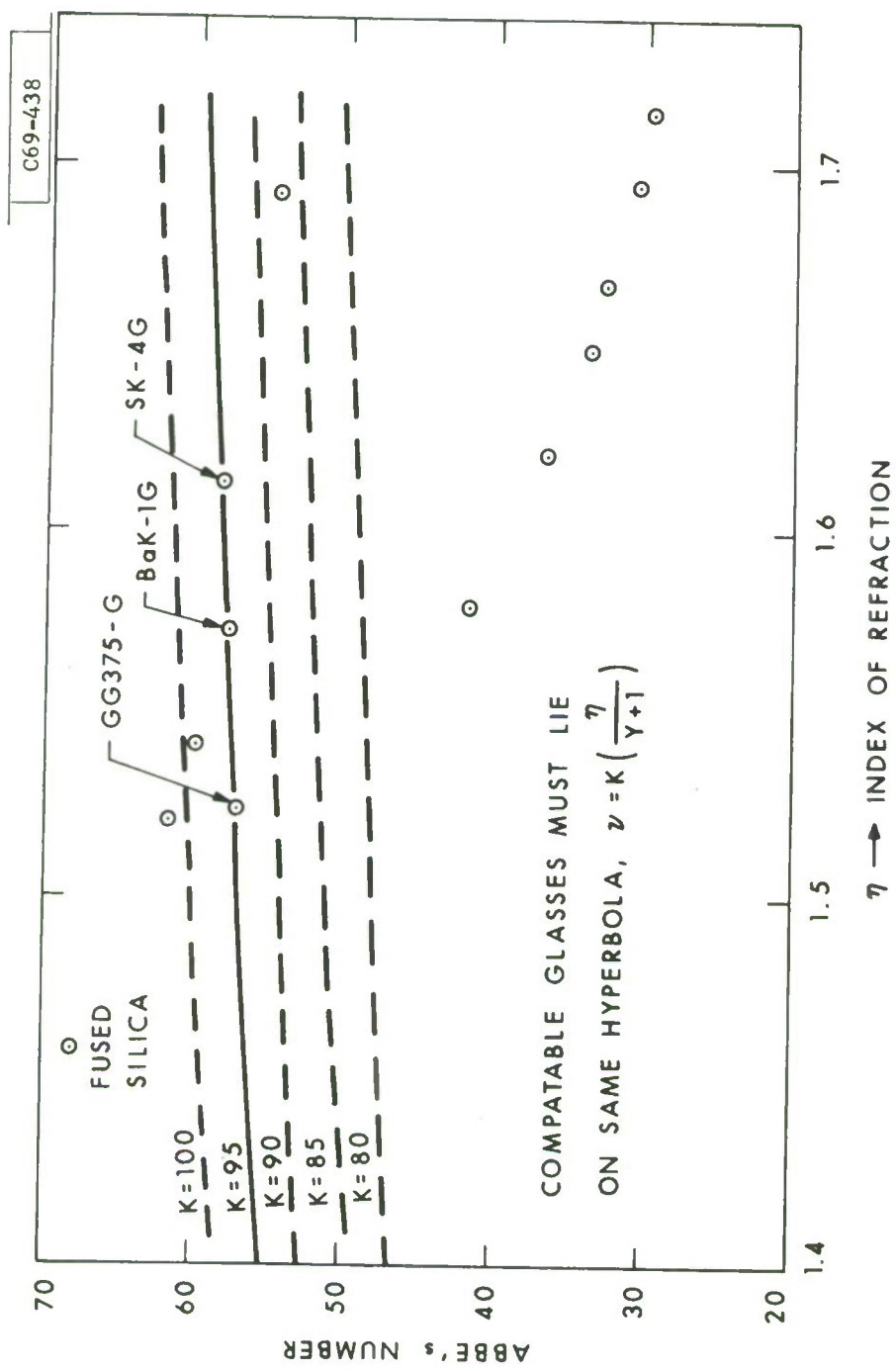


Fig. A-1. Parametric equation plots for achromatization.

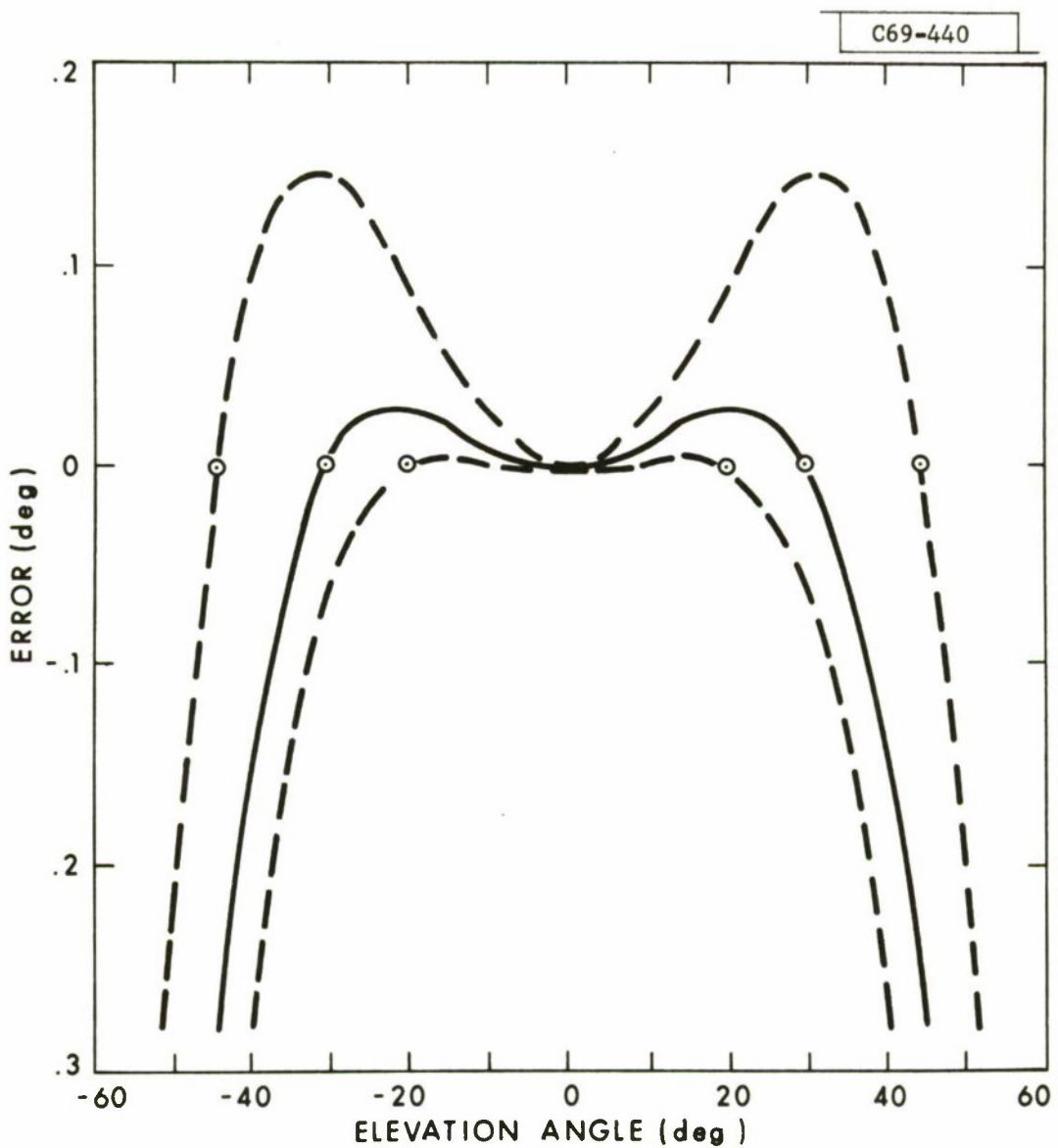


Fig. A-2. Glasses optimized for  $+30^\circ$ .

choosing the pair with smallest differences in indices. We did not choose, however, the glasses with the smallest differences for two reasons: it yielded a more rational design which was far less critical to the exact index, and did not require such a close match of dispersions. This decision was arbitrary, but we have so far no reason to regret it. In fact, all sun transit sensors aboard the LES-8 and -9 used this combination of glasses, and all were optimized for coincidence at  $30^{\circ}$  at the D line.

#### D. Sensor Design Optimized for Narrow Angle Operation

We next discuss a design which is optimized at the angle of plus or minus  $10^{\circ}$ . Here, generally speaking, the geometrical errors of even the half cell are negligible, compared to the chromatic spreads. The errors of the combined cell assembly, using push-pull connection of the cells would, in practice, be due to other factors such as fabrication tolerances and assembly of the units.

In Fig. A-3 we show the data for a half cell optimized at  $\pm 10^{\circ}\text{C}$ . When the sensor designs were finalized for the LES satellite, we also used a derivative of the design, miniaturized to fit a smaller package to operate within a gyro package.

#### E. Design of the Gyro Drift Sensor

The same prism unit was repackaged and recertified. However, where duplicate performance tests were performed at the Draper Laboratory they did not coincide with our earlier test results. The test apparatus equipment in particular were suspect. The difficulties, fortunately, proved to be in the

C69-442

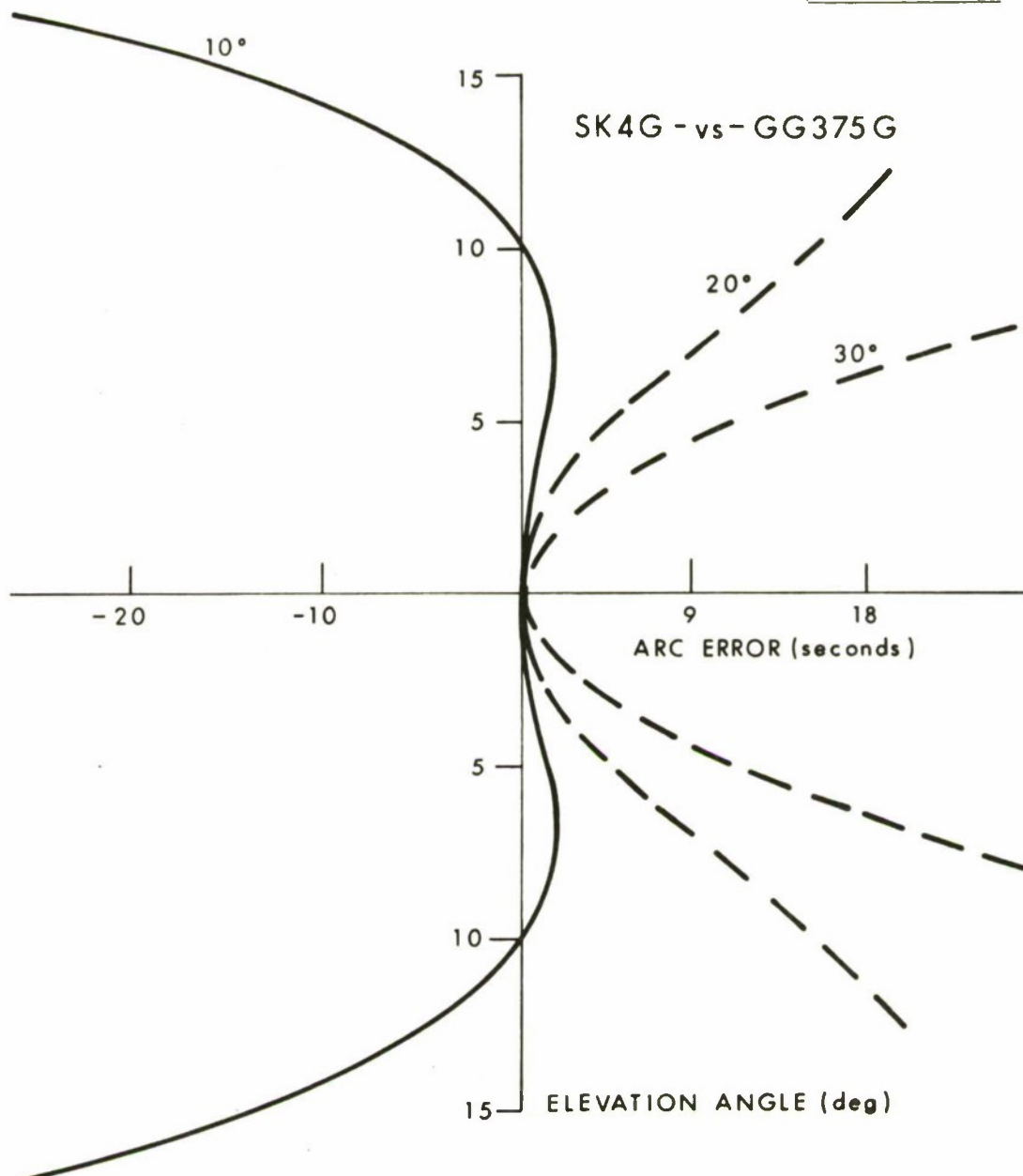


Fig. A-3. Glasses optimized for  $+10^\circ$ .

test equipment and not in the sensor. These subtle difficulties, which originated with the solar simulator, were discussed in the main body of this paper.

Fortunately, except for the need to redesign the sunshade, the performance of the original prism unit has proved to be sound in this more demanding application. Further work is needed to determine the ultimate accuracy limits of the sun transit sensor unit; this will require an investment in precision angular measurement apparatus beyond the level that we have so far required. In particular, we will require a precision turntable of modest angular capability, but extreme stability of the axis of the table, i.e., variations of the normal to the surface of the table must be controlled to one arc second or better.

#### F. Grey Program

```

C THIS STARTS PRINTOUT ON A NEW PAGE
200 IF(RN(1,1).GT.RN(2,1)) GO TO 202
Q=RN(2,1)
RN(2,1)=RN(1,1)
RN(1,1)=Q
Q=RN(2,2)
RN(2,2)=RN(1,2)
RN(1,2)=Q
C ROUTINE STARTING AT 200 INTERCHANGES GLASSES IF NECESSARY
202 CONTINUE
IF (RN(1,2).LE.0.) RN(1,2)=100.
C DEFAULT CHCICE FOR DISPERSION OF HIGHER INDEX GLASS
IF((RN(1,1)*RN(2,1)).GT.1.) GO TO 201
WRITE(W,101)
101 FORMAT(' FATAL DATA DEFAULT ')
C ONE OF THE REFRACTIVE INDICES WAS UNSPECIFIED
GO TO 1
201 IF(CV(1).LE.0.) CV(1)=20.
C DEFAULT CHOICE FOR CV(1) WHICH ALWAYS WORKS
IF(CV(2).LE.0.) CV(2)=30.
C DEFAULT CHOICE FOR CV(2) MATCHING EQUATORIAL ORBIT
C DEFAULT CHCICE FOR CV(3) FANS TO TWICE COOINCIDENCE ANGLE
IF(CV(3).LE.0.) CV(3)=2.0*CV(2)
IF(CV(4).LE.0.) CV(4)=CV(3)*.05
C OFTEN USED DEFAULT OPTION FOR CV(4) GIVING 20 RAYS IN FAN
M=CV(3)/CV(4)+1
WRITE(W,110) RN(1,1),RN(1,2),RN(2,1),RN(2,2),TITLE
110 FORMAT(1X, '1ST INDEX AND V',2F10.6,/1X,'2ND INDEX AND V',2F10.6,
1/1X,7A4)
WRITE(W,111)(CV(J),J=1,6)
111 FORMAT(1X,'START AT',F10.6/1X,'COINC AT',F10.6/1X,'FAN TO',F10.6/
1 1X,'INTERVALS OF',F10.6/1X,'SPECIFIED FIRST AND
1 SECOND PRISM ANGLES',2F10.6)
CV(1)=SIN(CV(1)/57.29578)
CV(2)=SIN(CV(2)/57.29578)
CV(3)=SIN(CV(3)/57.29578)
CV(4)=SIN(CV(4)/57.2958 )
C ABOVE FOUR EQUATIONS REPLACE ANGLES BY THEIR SINES
X(2)=SQRT(1.-CV(2)**2)
CALL ASOLV
C ASOLVE DETERMINES OPTIMAL ANGLES OF THE PRISM
CALL RAYFAN(M)
C RAYFAN(M) COMPUTES SUCCESSIVE AZIMUTHAL ERRORS IN DEGREES
IF((RN(2,2).EQ.0.).AND.(RN(1,2).EQ.0.)) GO TO 1
C WE ARE FINISHED WITH THESE GLASSES IF NO DISPERSIONS SUPPLIED
C WE NOW COMPUTE THE OPTIMAL SECOND DISPERSION
RASM=RN(1,1)
C WE THEREBY STORE RN(1,1)
RN(1,1)=RN(1,1)-(RN(1,1)-1.)/RN(1,2)
QXTG(1)=1.
QYTG(1)=0.
QZTG(1)=0.
CALL TRACE

```

```

COSI=QYTG(1)*A1(1)+QXTG(1)*A1(2)
SINI=SQRT(1.-COSI**2)
Q=SINI*RN(1,1)
RASP =-(RN(2,1)-1.)/(Q-RN(2,1))
C RASP IS THE CALCULATED OPTIMAL DISPERSION
WRITE(W,105) RASP
105 FORMAT(1X, ' RECIP. DISP. REQ. = ',F8.3)
RN(1,1) =RASM
C THUS WE RECALL RN(1,1)
IF(RN(2,2).NE.0.) GO TO 3
C IF SECOND DISPERSION WAS SUPPLIED, WE USE IT
C OTHERWISE, WE USE THE THEORETICAL OPTIMAL VALUE COMPUTED ABOVE
RN(2,2) =RASP
3 RN(2,1)=RN(2,1)-(RN(2,1)-1.)/RN(2,2)
RN(1,1)=RN(1,1)-(RN(1,1)-1.)/RN(1,2)
C ABOVE EQUATIONS INCREMENT INDICES TO SECOND COLOR
WRITE (W,130)
130 FORMAT(1X,'2ND COLOR')
CALL RAYFAN(M)
C WE ARE NOW REPOLOTTING THE ERROR CURVE FOR SECOND COLOR
C SECOND COLOR CORRESPONDS TO APPROX. WAVELENGTH OF ANGS.
GO TO 1
C WE GO TO NEXT PAIR OF GLASSES
999 CALL EXIT
END
SUBROUTINE ASOLV
C ASOLVE COMPUTES THE ANGLES OF THE PRISM FOR EXACT BALANCING OF
C *CURVATURE ERRORS. IT IS THE HEART OF THE DESIGN PROGRAM.
COMMON /EL/ RN(2,2),CV(6),W,R,Q,S1,S2,X(2),QXTG(49),QYTG(49),
*QZTG(49),B1(3),C5,A1(3),NDUM(3),C2,C3,C7,C8,C9,C1,C4,
*Q1,Q2,C3,Q4
INTEGER W,R
EPS=.1
B1(1)=0.
C2=CV(1)
DSIN=RN(2,1)/RN(1,1)
C5S=1.-DSIN**2
C5=SQRT(C5S)
7 NDUM(3)=-1
1 QXTG(1)=1.
IF(C2.GE.1.)GO TO 6
QYTG(1)=0.
QZTG(1)=0.
CALL TRACE
C WITH NDUM(2)=1 TRACE REFRACTS RAY THROUGH FIRST SURFACE. NOW
C SOLVE FOR SIN(I)=RN(1)/RN(2)
A1(1)= QXTG(1)*DSIN+QYTG(1)*C5
A1(2)=QXTG(1)*C5-QYTG(1)*DSIN
C A1(1)=DIRECTION COSINE OF NORMAL TO SECOND FACE.
NDUM(3)=NDUM(3)+1
QYTG(1)=0.
QZTG(1)=CV(2)
QXTG(1)=X(2)

```

```

      CALL TRACE
      S2= QYTG(1)*A1(1)+QXTG(1)*A1(2)
C      S2=COS(I)
      Q=1.-S2*S2
      S1=Q
      IF(S1.GT.0.) GO TO 5
      IF(NDUM(3).NE.0) GO TO 6
20    IF(EPS.GE.1.) GO TO 14
      C2=EPS
      EPS=EPS+.05
      GO TO 7
6     B1(1)=.5*B1(1)
      C2=C2-B1(1)
      IF(C2.GE.1.) GO TO 6
      NDUM(3)=NDUM(3)+1
      IF(NDUM(3).LT.20) GO TO 1
14   WRITE(W,100)
100  FORMAT( 'NC CONVERGENCE ')
      GO TO 10
5     B1(2)=CSIN-SQRT(S1)
      IF(ABS(B1(2)).LT.1.E-6)GO TO 10
      IF(NDUM(3).NE.0) GO TO 12
      B1(1)=.01
      GO TO 13
12   B1(1)=B1(1)*B1(2)/(B1(3)-B1(2))
13   B1(3)=B1(2)
      C2=C2+B1(1)
      IF(C2.LE.0.) GO TO 20
      IF(C2.GE.1.) GO TO 6
      IF(NDUM(3).GT.20) GO TO 14
      GO TO 1
10   A1(3)=57.29578*ARSIN(A1(1))
      C3=57.29578*ARSIN(C2)
      CQM =A1(3)-C3
      WRITE(W,101)A1(3),C3,CQM
101  FORMAT(1X,'OPTIMAL 1ST ANGLE,PHI(1)= ',F10.6/1X,
1     'OPTIMAL 2ND ANGLE,PHI(2)= ',F10.6/,
1     1X,'OPTIMAL PRISM ANGLE,PHI(3)= 'F10.6/)
      IF(CV(5).NE.0.) A1(3)=CV(5)
      IF(CV(6).NE.0.) C3=CV(6)
C     THUS, IF EITHER PRISM ANGLE IS SPECIFIED, THAT ANGLE WILL
C     BE USED IN THE COMPUTATION.
      RETURN
      END
      SUBROUTINE TRACE
C     SUBROUTINE TRACE TRACES A RAY THRU THE SYSTEM
      COMMON /EL/ RN(2,2),CV(6),W,R,Q,S1,S2,X(2),QXTG(49),QYTG(49),
      *QZTG(49),B1(3),C5,A1(3),NDUM(3),C2,C3,C7,C8,C9,C1,C4,
      *Q1,Q2,Q3,Q4
      INTEGER W,R
      S1=SQRT(1.-C2*C2)
      QYTG(1)=-QXTG(1)*C2/RN(1,1)
      QZTG(1)=QZTG(1)/RN(1,1)

```

```

S2=SQRT(1.-QYTG(1)**2-QZTG(1)**2)
QXTG(1)=S2*S1-C2*QYTG(1)
QYTG(1)=CYTG(1)*S1+C2*S2
RETURN
END
SUBROUTINE RAYFAN(M)
COMMON /EL/ RN(2,2),CV(6),W,R,Q,S1,S2,X(2),QXTG(49),CYTG(49),
*QZTG(49),B1(3),C5,A1(3),NDUM(3),C2,C3,C7,C8,C9,C1,C4,
*Q1,Q2,Q3,Q4
INTEGER W,R
CS=CV(4)/RN(2,1)
C7=SQRT(1.-C2*C2)
C9=0.
C8=A1(2)
DO 1 J=1,M
QZTG(J)=C9
QXTG(J)=SQRT(1.-C9*C9)
QZTG(J)=C9*RN(2,1)/RN(1,1)
QYTG(J)=-QXTG(J)*          RN(2,1)/RN(1,1)
QXTG(J)=      (1.-QYTG(J)**2-QZTG(J)**2)
IF(QXTG(J).LE.0.) GO TO 3
QXTG(J)=SQRT(QXTG(J))
QYTG(J)=CYTG(J)*C8+A1(1)*QXTG(J)
QXTG(J)=      (1.-QYTG(J)**2-QZTG(J)**2)
IF(QXTG(J).LE.0.) GO TO 3
QXTG(J)=SQRT(QXTG(J))
QYTG(J)=CYTG(J)*C7-QXTG(J)*C2
QXTG(J)=      (1.-QYTG(J)**2-QZTG(J)**2)
IF(QXTG(J).LE.0.) GO TO 3
QXTG(J)=SQRT(QXTG(J))
QYTG(J)=CYTG(J)*RN(1,1)
QZTG(J)=QZTG(J)*RN(1,1)
QXTG(J)=      (1.-QYTG(J)**2-QZTG(J)**2)
IF(QXTG(J).LE.0.) GO TO 3
QXTG(J)=SQRT(QXTG(J))
QYTG(J)=CYTG(J)*C7+QXTG(J)*C2
QYTG(J)=CYTG(J)*57.29578
QZTG(J)=ARSIN(QZTG(J))*57.29578
C9=C9+CS
1  CONTINUE
4  WRITE(W,102)
102 FORMAT(1X,'ELEVATION AND AZIMUTHAL ERRORS (IN AIR)')
DO 2 J=1,M
2  WRITE(W,100)QZTG(J),QYTG(J)
100 FORMAT(5X,2F10.6)
RETURN
3  M=J
GO TO 4
END

```

G. Sample Calculations from Grey Program

1ST INDEX AND V    1.600000100.000000  
 2ND INDEX AND V    1.500000080.000000

NOTE: Here we specify both indices and both dispersions, i.e., v values.

START AT 20.000000  
 CCINC AT 30.000000  
 FAN TO 60.000000  
 INTERVALS OF 3.000000  
 SPECIFIED FIRST AND  
 OPTIMAL 1ST ANGLE, PHI(1) = 77.440399  
 OPTIMAL 2ND ANGLE, PHI(2) = 20.369568  
 OPTIMAL PRISM ANGLE, PHI(3) = 57.070831

SECOND PRISM ANGLES 0.0    0.0

ELEVATION AND AZIMUTHAL ERROR (IN AIR)

C.C	0.0
2.999996	0.001240
6.008246	0.004774
9.033242	0.009904
12.063878	0.016488
15.109725	0.023079
18.301361	0.026304
21.490738	0.030347
24.751709	0.026385
28.100708	0.013128
31.557816	-0.014193
35.148285	-0.062315
38.904968	-0.140278
42.872269	-0.261644
47.113419	-0.446783
51.724197	-0.728269
56.863846	-1.164461
62.836807	-1.873446
70.397980	-3.180760
C.994382	-0.143154

FECIE. EISE. REQ. = 96.875 ← It still computes the optional disp.  
 2ND COLOR

ELEVATION AND AZIMUTHAL ERROR (IN AIR)

C.C	0.186645
2.999996	0.188025
6.008250	0.191894
9.033245	0.197802
12.063878	0.205151
15.109725	0.212856
18.301361	0.219621
21.490738	0.223357
24.751694	0.221701
28.100693	0.210896
31.557785	0.186372
35.148254	0.141675
38.904922	0.067639
42.872238	-0.049112
47.113373	-0.228794
51.724167	-0.503873
56.863800	-0.931887
62.836746	-1.630113
70.397873	-2.918822
C.994361	-0.138950

These errors, computed for the second color, are large, even for 0.0 elevation, because the dispersions are much too far apart.

1ST INDEX AND V 1.600000100.000000 ← NOTE: Here we specify only  
2ND INDEX AND V 1.500000 0.0 the first dispersion.

START AT 20.00000  
CCINC AT 30.00000  
FAN TO 60.00000  
INTERVALS OF 3.00000  
SPECIFIED FIRST AND SECOND PRISM ANGLES 0.0 C.0  
OPTIMAL 1ST ANGLE, PHI(1) = 77.440395  
OPTIMAL 2ND ANGLE, PHI(2) = 20.369568  
OPTIMAL PRISM ANGLE, PHI(3) = 57.070831

ELEVATION AND AZIMUTHAL ERRORS (IN AIR)

C.C	0.0
2.999996	0.001240
6.000246	0.004774
9.033242	0.009904
12.083878	0.016488
15.169725	0.023079
18.301361	0.028304
21.490738	0.030347
24.751709	0.026385
28.100708	0.013128
31.557816	-0.014193
35.148285	-0.062315
38.904968	-0.140278
42.872269	-0.261644
47.113419	-0.446783
51.724197	-0.728269
56.863846	-1.164461
62.836807	-1.873446
70.397980	-3.180760
C.994382	-0.143154

REC'D. DISP. REQ. = 96.875 ←  
2ND CCINC

ELEVATION AND AZIMUTHAL ERRORS (IN AIR)

C.C	0.000120
2.999996	0.001438
6.000244	0.005269
9.033238	0.010993
12.083878	0.018209
15.169725	0.025801
18.301361	0.032317
21.490738	0.035729
24.751709	0.033663
28.100693	0.022526
31.557800	-0.002561
35.148285	-0.047842
38.904953	-0.122614
42.872269	-0.240508
47.113403	-0.421341
51.724182	-0.698066
56.863831	-1.128484
62.836746	-1.830521
70.397934	-3.128308
C.994382	-0.142204

SAMPLE CALCULATION

The program computes the optimal second dispersion and uses same to achieve negligible color error at zero elevation.

UNCLASSIFIED

**SECURITY CLASSIFICATION OF THIS PAGE (When Data Entered)**